Mean occupancy time: linking mechanistic movement models, population dynamics and landscape ecology to population persistence

Christina A. Cobbold & Frithjof Lutscher

Journal of Mathematical Biology

ISSN 0303-6812
Volume 68
Number 3

J. Math. Biol. (2014) 68:549-579
DOI 10.1007/s00285-013-0642-1

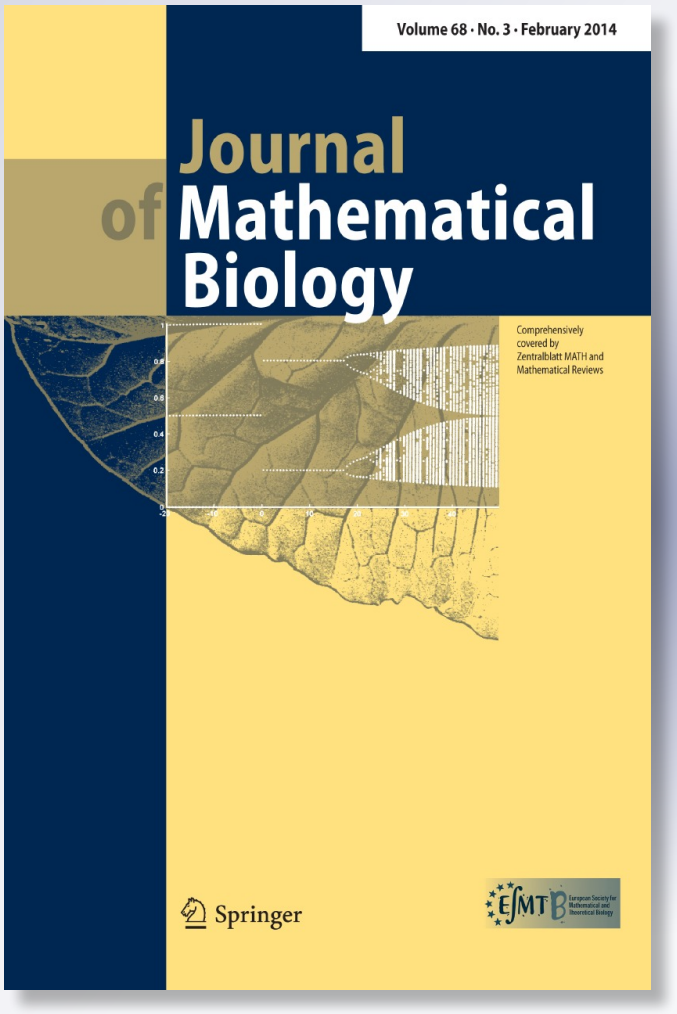

Springer

J. Math. Biol. (2014) 68:549–579
DOI 10.1007/s00285-013-0642-1

Mathematical Biology

Mean occupancy time: linking mechanistic movement models, population dynamics and landscape ecology to population persistence

Christina A. Cobbold · Frithjof Lutscher

Received: 26 May 2012 / Revised: 17 December 2012 / Published online: 20 January 2013

Abstract Reaction–diffusion models for the dynamics of a biological population in a fragmented landscape can incorporate detailed descriptions of movement and behavior, but are difficult to analyze and hard to parameterize. Patch models, on the other hand, are fairly easy to analyze and can be parameterized reasonably well, but miss many details of the movement process within and between patches. We develop a framework to scale up from a reaction–diffusion process to a patch model and, in particular, to determine movement rates between patches based on behavioral rules for individuals. Our approach is based on the mean occupancy time, the mean time that an individuals spends in a certain area of the landscape before it exits that area or dies. We illustrate our approach using several different landscape configurations. We demonstrate that the resulting patch model most closely captures persistence conditions and steady state densities as compared with the reaction–diffusion model.

Keywords Spatial ecology · Patchy landscape · Model reduction · Reaction–diffusion equation · Patch model

Mathematics Subject Classification (2000) 92B05 · 35K57 · 35K25 · 60J70

C. A. Cobbold (✉)
School of Mathematics and Statistics,
University of Glasgow, Glasgow, UK
e-mail: cc@maths.gla.ac.uk

F. Lutscher
Department of Mathematics and Statistics,
University of Ottawa, Ottawa, ON, Canada
e-mail: flutsche@uottawa.ca

1 Introduction

The persistence of biological populations in a given landscape under certain circumstances is one of the foremost concerns in conservation biology. The likelihood of a population to persist depends on the interplay between the life cycle of individuals, i.e. how they grow, reproduce and die, and their dispersal ability, i.e. how they utilize spatially distributed resources. Natural and human disturbances of landscapes have led to increased rates of habitat fragmentation and degradation. Consequently, many species encounter a landscape consisting of patches of variable quality and separated by more or less suitable 'matrix' habitat. Various modeling approaches are used to help gain insight into population persistence in such landscapes and to inform management options, such a reserve design.

Reaction–diffusion equations (RDEs) in the broadest sense (e.g. including advection and taxis), are the 'workhorse' in spatial ecology (Othmer et al. 1997; Cantrell and Cosner 2003). In these equations, the evolution of a continuous density of individuals is tracked over time. Individual mechanisms and processes are incorporated at a fine scale; movement is modeled as a random walk. The simplest and original question of population persistence is the 'critical patch size problem' that dates back to (Skellam 1951; Kierstead and Slobodkin 1953), where it was treated as an eigenvalue problem of a reaction–diffusion equation.

The versatility of reaction–diffusion equations comes at a price. Analyzing such equations with spatially variable coefficient functions is hard, and sometimes even numerical simulations of solutions can be demanding. In addition, data requirements to fit spatially varying coefficient functions are very high.

Landscape ecologists frequently view landscapes as collections of patches of different habitat quality. Each patch is essentially homogeneous within but significantly different from its surroundings. Accordingly, models for populations that live in a patchy landscape typically track the dynamics within a patch as an ordinary differential equation and link patches via emigration and immigration by first-order gain and loss terms. Such patch models, sometimes referred to as discrete-diffusion models, are frequently studied in the literature. Two-patch models are particularly attractive since their behavior can be displayed as a phase-plane portrait, but even multi-patch models are still much easier to analyze and parameterize than corresponding reaction–diffusion models. Our overarching goal here is to translate reaction–diffusion models into patch models in the 'best' possible way.

Several questions emerge immediately. Since patch models necessarily aggregate information, how close are their predictions to those of corresponding reaction–diffusion models with more details (Cantrell et al. 2012)? Or: how do the physical dimensions of a corridor and the diffusion rate there determine the discrete diffusion rate between two patches linked by the corridor (Wakano et al. 2011)? Or, more generally, given a reaction–diffusion equation in a patchy landscape, how does one define a patch model that most closely reflects the reaction–diffusion model? In particular, how does one scale up from individual random walks in a patchy landscape to a migration rate between two patches? The goal of this work is to develop a formalism that answers these questions and provides an algorithmic (computational) procedure to derive patch models.

The key ingredient in our modeling framework is the so-called *mean occupancy time*. This quantity gives the average time that an individual following a random walk spends inside a certain region before it either crosses the boundary of the region or dies. Our work is inspired by related recent progress for integrodifference equations. These discrete-time analogues to reaction–diffusion equations can be related to discrete-time patch model via the 'average dispersal success' approximation (Van Kirk and Lewis 1997; Lutscher and Lewis 2004; Fagan and Lutscher 2006). This technique uses spatial averaging and Taylor series approximation to find an approximate persistence condition, and suggests point- or area-release experiments to parameterize the models. Here, we use spatial averaging and occupancy times to obtain ODE approximations to RDE models. We answer the question of how these two modeling approaches are connected.

In the following section, we present our formalism using the original critical patch size problem as an example where all calculations can be carried out explicitly. Then we present the general formulation of the theory in Sect. 3. We illustrate the scope of our approach, using several well-known models in spatial ecology (Sect. 4). We give the detailed derivations in Sect. 5 and close with a discussion.

2 Motivating example

We present the crucial ideas in a heuristic way, using a particular version of the KISS model as the most basic example, named after Kierstead and Slobodkin (1953) and Skellam (1951). We assume that a population of individuals resides and moves in the one-dimensional habitat of length L. We choose the domain to be $\Omega = [-l, l]$ with $l = L/2$, so that we can use symmetry around $x = 0$ later. We assume that individuals reproduce with per capita rate b, and move randomly with diffusion coefficient D. We assume that the boundary of the habitat is hostile and that the per capita death rate is much smaller than the loss rate of individuals through the boundary of the habitat, so that we ignore death for the moment. Then the equation for the population density $u(x, t)$ reads

$$\frac{\partial u}{\partial t} = D\frac{\partial^2 u}{\partial x^2} + f(u), \qquad x \in \Omega, \qquad u(\pm l, t) = 0, \tag{1}$$

with birth function $f(u) = bu$. The critical patch size for this model is $L_c = \pi\sqrt{\frac{D}{b}}$. A population inhabiting a patch of size less than L_c will go extinct (Skellam 1951; Kot 2001).

If we simply average (1) over the patch, then the resulting equation for $\bar{u} = \frac{1}{L}\int_\Omega u(t, x)dx$ is not closed since the derivative of u at the boundary appears. We seek an approximation for $\bar{u}$ that satisfies a simple equation for the population density on the patch. These "patch dynamics" for this model should be particularly simple since there is only one patch and only emigration but no immigration. Hence, the corresponding patch model for the average population density on the patch, $U(t)$, should have the form

$$\dot{U} = -MU + f(U). \tag{2}$$

Here $M > 0$ is the rate at which individuals leave the patch. Accordingly, $1/M$ is the mean residence time in the patch before reaching the hostile boundary. We now connect M to the movement model underlying (1).

We define the *mean first passage time* $T(x)$ as the mean time that it takes an individual to reach the boundary of Ω from location x, when moving randomly with diffusion coefficient D (Redner 2001). Then T is the solution of the boundary value problem (McKenzie et al. 2009)

$$DT''(x) = -1, \quad x \in \Omega, \qquad T(\pm l) = 0. \tag{3}$$

The solution has to be symmetric with respect to $x \mapsto -x$; it is given by $T(x) = \frac{L^2}{8D} - \frac{x^2}{2D}$. The spatially averaged mean first passage time is then

$$\overline{T} = \frac{1}{L}\int_{-l}^{l} T(x)dx = \frac{L^2}{12D}. \tag{4}$$

We assume here that starting location, x, is distributed uniformly across the domain. This is a reasonable null hypothesis and is consistent with the fact that the steady state distribution for the population is almost uniform in the interior of the domain. Hence, the natural candidate for the patch emigration rate is $M = 1/\overline{T}$.

The population persistence threshold for (2) is $b - M > 0$; given the dependence of M on L and D, this condition now translates into a critical patch size of

$$\overline{T} > \overline{T}_c = 1/b, \quad \text{or} \quad L > \hat{L}_c = \sqrt{12}\sqrt{\frac{D}{b}}. \tag{5}$$

Since $\sqrt{12} \approx 3.464 > \pi$, critical patch size $\hat{L}_c$ predicted by the patch approximation exceeds the critical size L_c from the spatially explicit KISS model by about 10 %. The persistence condition in terms of residence time ($\overline{T}b > 1$) is the natural condition that an individual needs to stay in the domain long enough to replace itself before leaving the domain.

Since a constant per capita birth rate is an unrealistic assumption at higher population densities, we next consider a birth or fecundity function $f(u) > 0$ that saturates at high density, for example

$$f(u) = \frac{bu}{1 + \alpha u} \tag{6}$$

with maximum birth rate b. Parameter α determines how fast the birth rate declines with density. Then model (1) has a unique positive steady state, given by

$$Du^*_{xx} + f(u^*) = 0, \tag{7}$$

provided $L > L_c = \pi\sqrt{\frac{D}{b}}$. The corresponding patch approximation has the steady state equation

$$U^* = \overline{T} f(U^*). \tag{8}$$

We will show in the next section, that U^* is a reasonable approximation to the spatial average $\bar{u}^*$ of $u^*(x)$.

The mean first passage time, $T(x)$, is smaller near the boundary of the habitat than in the center. We use this information to obtain a heuristic approximation to the steady state profile $u^*(x)$. In Eq. (1), we replace Du_{xx} with $(-1/T(x))u$, indicating that the loss rate from the center of the domain is smaller than near the perimeter. (We have temporarily ignored the fact that T is zero at the boundary.) Formally solving for a steady state gives $u^*(x) = T(x) f(u^*)$. Together with the result that $u^*(x)$ is close to its spatial average U^*, we obtain the approximation

$$u^*(x) \approx T(x) f(U^*). \tag{9}$$

We will make all these heuristic arguments more rigorous in subsequent sections.

In the final step, we drop the assumption that the death rate of individuals is small compared to loss through movement across the boundary. The simplest way to include a death rate into the equation would be to think of the function f as net reproduction - birth minus death, - for example $f(u) = bu/(1 + \alpha u) - mu$. It turns out that there are at least three problems with this approach.

1. The approximation (9) of the spatial profile of the steady state is not particularly close (see Figs. 3, 4).
2. The approach requires that individuals eventually leave the area of consideration since otherwise the mean residence time approaches infinity. Hence the approach does not generalize to no-flux conditions or habitats consisting of multiple patches, surrounded by insurmountable boundaries.
3. The approach violates basic bookkeeping rules. An individual can only die at the location where it currently resides and not anywhere else. Including death into the function f would mean that in the patch approximation, individuals die where they are on average rather than where they are actually.

To remedy the situation we include mortality as a Poisson process with intensity m into the movement operator. Instead of the mean first passage time, we define the *mean occupancy time* as the mean time that an individual is alive within the habitat, i.e. the mean time before it leaves *or* dies. For an individual moving randomly with diffusive rate D and mortality m, the occupancy time for starting location $x \in \Omega$ is given by the equation (Ovaskainen and Cornell 2003)

$$DT''(x) - mT(x) = -1, \quad x \in \Omega, \qquad T(\pm l) = 0, \tag{10}$$

where we assumed hostile boundaries again. The solution has to be symmetric with respect to $x \mapsto -x$; it is given by

$$T(x) = \frac{1}{m}\left[1 - \cosh\left(l\sqrt{\frac{m}{D}}\right)^{-1} \cosh\left(x\sqrt{\frac{m}{D}}\right)\right] \tag{11}$$

with mean occupancy time

$$\overline{T} = \frac{1}{m}\left[1 - \frac{1}{l}\sqrt{\frac{D}{m}}\tanh\left(l\sqrt{\frac{m}{D}}\right)\right]. \tag{12}$$

We call the resulting approximations (2, 9) with $M = 1/\overline{T}$ and $T(x)$, $\overline{T}$ as in (11,12) the *mean occupancy time approximation* of (1), or MOT approximation for short. The critical patch size $\hat{L}_c$ is now given by $b = M = 1/\overline{T}$, which is the unique positive solution of the transcendental equation

$$\frac{L}{2}\sqrt{\frac{m}{D}} = \frac{b}{b-m}\tanh\left(\frac{L}{2}\sqrt{\frac{m}{D}}\right). \tag{13}$$

We illustrate several aspects of all of the above heuristic approximations in several plots for a somewhat more general model in Sect. 4.1. But first, we present the general theoretical concept and derivations.

3 General theory

In general, a reaction–diffusion equation for the density $u(\mathbf{x}, t)$ of a single species at time t at location $\mathbf{x}$ in some spatial domain $\Omega \subset \mathbb{R}^n$ can be written as

$$\frac{\partial u}{\partial t} = \mathcal{M}[u](\mathbf{x}) + \mathcal{F}(u, \mathbf{x}), \quad u(\mathbf{x}, t) = u_0(\mathbf{x}). \tag{14}$$

We denote $\mathcal{M}$ as the operator describing individual movement and mortality, where movement is modeled as the negative divergence of the population flux $\mathbf{J}$ that may depend on population density, its gradient and explicitly on spatial location. Local fecundity is given by $\mathcal{F}(u, \mathbf{x})$, where explicit dependence on spatial location can reflect habitat heterogeneity. At the boundary $\partial\Omega$ of the spatial domain, the boundary condition relates population flux to density as $\alpha(\mathbf{x}) \cdot \mathbf{J} = u(\mathbf{x}, t)$ on $\partial\Omega \times (0, \infty)$.

Landscape ecology typically considers a habitat as an assemblage of patches that are assumed homogeneous within but different from their respective surroundings. In the simplest case, there is a single good patch located in less favorable matrix habitat; more generally, there can be any finite number of patches Ω_j, $j = 1 \ldots n$. The population density in patch j, denoted by U_j, changes due to migration between patches ($\mathbf{M}$), and growth within each patch ($\mathbf{F} = (F_1, \ldots, F_n)'$) according to

$$\dot{\mathbf{U}} = \mathbf{M}\mathbf{U} + \mathbf{F}(\mathbf{U}). \tag{15}$$

Here, $\mathbf{U} = (U_1, \ldots, U_n)'$ denotes the column vector of population densities and $\frac{d}{dt} = \dot{}$ denotes the time derivative. The diagonal elements of matrix $\mathbf{M} = (m_{ij})$ are negative and describe emigration from a patch, whereas the (non-negative) off-diagonal elements give the rates of migration from one patch to another. In the case of a single patch in a hostile landscape, there is no immigration. Typically, mortality is included in the function $\mathbf{F}$, but it can easily be placed into matrix $\mathbf{M}$ as additional diagonal entries.

In the following, we derive a formalism by which we can relate individual movement behavior and growth functions in the spatially explicit equation (14) to the movement rates and growth functions in the spatially implicit equation (15). In other words, we answer the main question at the heart of this work:

Question Given $\mathcal{M}$ and $\mathcal{F}$ in a patchy landscape, how can we define $\mathbf{M}$ and $\mathbf{F}$ in such a way that (15) most closely captures (14)?

The crucial link between the two equations are spatially averaged occupancy times derived from the movement operator $\mathcal{M}$. We show that with this formalism, the spatially implicit equation approximates to first order the spatial averages of the spatially explicit equation at steady state, and it approximates the population persistence conditions to the same degree. Furthermore, in the case of a single patch, we derive an approximation to the spatial profile of the steady state of (14) based on occupancy times.

The mean occupancy time (MOT) is the spatially averaged expected time that an individual is located within a certain patch and alive. When there is no mortality, this quantity is better known as the average mean first passage time (MFPT). It can be obtained in several different ways: (i) from experimental data directly (Schultz and Crone 2001), (ii) from first passage probabilities (Redner 2001), (iii) from the adjoint of the movement operator (Ovaskainen and Cornell 2003; Ovaskainen 2008), and (iv) from an explicit random walk derivation (McKenzie et al. 2009). We will use (ii) to derive the approximations and (iii) for calculations in examples. We provide a brief description of these two approaches.

We denote G as the Green's function of the operator $\mathcal{M}$. Furthermore, we denote $S(\mathbf{y}, t)$ as the probability that an individual starting at location $\mathbf{y} \in \Omega$ is still in the domain and alive at time t. Using the Green's function, we can express $S(\mathbf{y}, t)$ as

$$S(\mathbf{y}, t) = \int_{\Omega} G(\mathbf{x}, \mathbf{y}, t)\, d\mathbf{x}.$$

Similarly, the first passage probability, $F(\mathbf{y}, t)$ is the probability that an individual starts at $\mathbf{y}$ and dies or reaches the boundary for the first time at time t. This quantity can be written as

$$\int_0^t F(\mathbf{y}, \tau) d\tau = 1 - S(\mathbf{y}, t).$$

Thus, the occupancy time for an individual starting at location $\mathbf{y}$ is given by

$$T(\mathbf{y}) = \int_0^\infty tF(\mathbf{y},t)\,dt = -\int_0^\infty t\frac{\partial S}{\partial t}\,dt = \int_0^\infty\int_\Omega G(\mathbf{x},\mathbf{y},t)\,d\mathbf{x}\,dt. \tag{16}$$

As a necessary condition, we require $\lim_{t\to\infty} S(\mathbf{y},t) = 0$, i.e., individuals will eventually die or exit the domain with probability 1. In particular, if there is no mortality, then the boundary has to be "leaky".

Explicit calculations use the adjoint operator of $\mathcal{M}$, as first presented and explained in detail by Ovaskainen and Cornell (2003) and later applied in Ovaskainen (2008). The occupancy time density

$$B(\mathbf{x},\mathbf{y}) = \int_0^\infty G(\mathbf{x},\mathbf{y},t)dt. \tag{17}$$

satisfies the equation $\mathcal{M}B = -\delta$, the delta-distribution. The mean time that an individual originally located at $\mathbf{y}$ is alive and in Ω is given by the integral of B over Ω. Using the definition of T as well as the relationship $\mathcal{M}B = -\delta$, we find

$$\int_\Omega B(\mathbf{x},\mathbf{y})d\mathbf{x} = T(\mathbf{y}) = -\int_\Omega T(\mathbf{x})\mathcal{M}B(\cdot,\mathbf{y})d\mathbf{x} = -\int_\Omega B(\mathbf{x},\mathbf{y})\mathcal{M}^*T\,d\mathbf{x}. \tag{18}$$

Here $\mathcal{M}^*$ denotes the adjoint of $\mathcal{M}$. Therefore, T satisfies the equation

$$\mathcal{M}^*T = -1,\ \mathbf{x}\in\Omega. \tag{19}$$

When the total habitat is subdivided into n distinct patches $\Omega_j,\ j = 1,\ldots,n$ whose union is all of Ω, i.e. $\Omega = \dot\cup_j\Omega_j$, then we will also need the occupancy time in each patch Ω_i, denoted by T_{Ω_i}. Similar to the above, this quantity is obtained as the solution of (Ovaskainen and Cornell (2003))

$$\mathcal{M}^*T_{\Omega_i} = -1,\ \mathbf{x}\in\Omega_i,\quad \mathcal{M}^*T_{\Omega_i} = 0,\ \mathbf{x}\notin\Omega_i. \tag{20}$$

With this notation, we have $T_\Omega = T$.

3.1 The case of a single patch

We consider Eq. (14) on a bounded connected patch Ω. We define the MOT patch model as

$$\dot U = -\frac{1}{\overline{T}}U + \mathcal{F}(U), \tag{21}$$

with $\mathcal{F}$ as in (14) and $\overline{T}$ the spatial average of $T(\mathbf{x})$ from (19). Then the following approximations hold to lowest order (see Sect. 5).

1. The spatial average of a steady state of (14) is approximated by a steady state of (21).
2. If movement is isotropic then the steady state of (14) is approximated by $u^*(\mathbf{x}) \approx \mathcal{F}(\bar{u}^*)T(\mathbf{x})$.
3. If $\mathcal{F}(u) = ru$ is linear, then the dominant eigenvalue of (21) is a good approximation of the dominant eigenvalue of (14).

As a consequence of the above, the persistence condition for the spatially implicit equation is a good approximation of the persistence condition of the spatially explicit equation; and the same holds true for the stability condition for a positive steady state.

In Sect. 4 we will illustrate how to calculate the occupancy time approximation and how well this approximation works with a number of different examples.

3.2 The case of multiple patches

When the domain is not homogeneous, we consider a subdivision into n distinct patches $\Omega_j,\ j = 1, \ldots, n$ that make up all of Ω, i.e. $\Omega = \dot{\cup}_j \Omega_j$. Since each patch is assumed homogeneous, we set the population dynamics on each patch as $F_i(u) = \mathcal{F}(u, \mathbf{x})$ for $\mathbf{x} \in \Omega_i$. Then the MOT approximation of (14) is

$$\dot{\mathbf{U}} = -\mathcal{T}^{-1}\mathbf{U} + \mathbf{F}(\mathbf{U}), \tag{22}$$

where matrix $\mathcal{T} = (T_{ij}) = -\mathbf{M}^{-1}$ has entries

$$T_{ij} = \frac{|\Omega_j|}{|\Omega_i|}\,\frac{1}{|\Omega_j|}\int_{\Omega_j} T_{\Omega_i}(\mathbf{y})d\mathbf{y}. \tag{23}$$

Hence, T_{ij} is the occupancy time in Ω_i, spatially averaged over the starting patch Ω_j, multiplied by the fraction of the respective patch areas. This fraction is the conversion factor from densities in Ω_j into densities in Ω_i. The notation $|\Omega_j|$ stands for the measure of the set Ω_j; i.e. the length for an interval and the area for a two-dimensional domain.

In Sect. 5.3 we show that

1. the patch averages of a steady state of the spatially explicit Eq. (14) are approximated by a steady state of (22); and
2. the dominant eigenvalue of (22) when $\mathcal{F}$ is linear is a good approximation of the dominant eigenvalue of (14).

In the following section, we illustrate our approach, using a number of well-established models in spatial ecology.

4 Examples and results

We demonstrate the scope of our approach by revisiting some classical models in spatial ecology and comparing our approximation results to the analytically available results. We focus mostly on the conservation issue of population persistence as a function of habitat size and other parameters describing individual movement. We assume that population growth does not exhibit an Allee effect and define population persistence as the ability of the population to invade new habitat and grow at low density.

4.1 Single patch with movement behavior at the boundary

Hostile boundary conditions, as in the introductory example, may apply to a plant species with wind borne seeds on an island surrounded by ocean. Many animals, however, perceive habitat boundaries and modify their movement behavior so that they only leave a good patch with probability p and stay with probability $1-p$. Van Kirk and Lewis (1999) showed that this situation can be modeled by a diffusion equation with mixed boundary conditions. We adopt the boundary condition of Van Kirk and Lewis (1999), but depending on the assumptions made about how the individual encounters the boundary alternative conditions can be constructed (see for example Cantrell and Cosner 2007; Singer et al. 2008). Our model reads

$$u_t = Du_{xx} + \frac{bu}{1+\alpha u} - mu, \qquad x \in (-l, l) \tag{24}$$

$$u_x(-l,t) = \chi u(l,t), \quad u_x(l,t) = -\chi u(l,t), \tag{25}$$

where $r = b - m$ is the net intrinsic growth rate and $\chi = \frac{p}{1-p}\sqrt{\frac{r}{D}}$.

The resulting critical domain size is (Ludwig et al. 1979)

$$L_c = 2\sqrt{\frac{D}{r}} \arctan\left(\frac{p}{1-p}\right). \tag{26}$$

The occupancy time satisfies the equation in (10) with boundary conditions in (25), namely

$$T(x) = \frac{1}{m}\left[1 - \left[\cosh\left(l\sqrt{\frac{m}{D}}\right) + \frac{1}{\chi}\sqrt{\frac{m}{D}}\sinh\left(l\sqrt{\frac{m}{D}}\right)\right]^{-1}\cosh\left(\sqrt{\frac{m}{D}}x\right)\right], \tag{27}$$

and

$$\overline{T} = \frac{1}{m}\left[1 - \frac{1}{l}\sqrt{\frac{D}{m}}\tanh\left(l\sqrt{\frac{m}{D}}\right)\left(1 + \frac{1}{\chi}\sqrt{\frac{m}{D}}\tanh\left(l\sqrt{\frac{m}{D}}\right)\right)^{-1}\right]. \tag{28}$$

The corresponding critical patch size is given by the unique positive solution of $b\overline{T} = 1$ or

$$\frac{L}{2}\sqrt{\frac{m}{D}}\left[1 + \frac{1}{\chi}\sqrt{\frac{m}{D}}\tanh\left(\frac{L}{2}\sqrt{\frac{m}{D}}\right)\right] = \frac{b}{r}\tanh\left(\frac{L}{2}\sqrt{\frac{m}{D}}\right). \tag{29}$$

In the limit of hostile boundary conditions ($p \to 1$) we recover the expressions for L_c and $\hat{L}_c$ from Sect. 2.

Finally, we consider the MOT approximation (9) to the steady state of the PDE model (24) and (25). The explicit expression of u^* is given by

$$u^*(x) = \left(\frac{b\overline{T} - 1}{\alpha\overline{T}}\right)T(x), \tag{30}$$

where $\overline{T}$ and $T(x)$ are from (28) and (27).

In two spatial dimensions, the MOT approach works the same way, but the calculations become more difficult. In the simplest case, the domain is a disc of radius R. Assuming a hostile boundary condition, the KISS model (1) has critical radius $R_c = \beta_1\sqrt{\frac{D}{b-m}}$ (e.g. Kot 2001, p. 288), where β_1 is the first zero of the zero-order Bessel function of the first kind, J_0.

The mean occupancy time equation on a disc of radius R with hostile boundary is radially symmetric and can be written in polar coordinates as

$$D\left(T'' + \frac{1}{\rho}T'\right) - mT = -1, \quad 0 \le \rho \le R, \quad T(R) = 0, \quad \rho^2 = x^2 + y^2. \tag{31}$$

The solution is given explicitly by a Bessel function with complex argument as

$$T(\rho) = \frac{1}{m}\left(1 - \frac{J_0\left(\mathrm{i}\sqrt{\frac{m}{D}}\rho\right)}{J_0\left(\mathrm{i}\sqrt{\frac{m}{D}}R\right)}\right). \tag{32}$$

However, there is no closed form explicit expression for $\overline{T}$ in this case. On a rectangular domain, the equation for T can be solved in terms of Fourier series, so that, again, numerical tools are required to evaluate the resulting expressions; see Appendix B.

4.2 Partitioning the net growth rate

In Sect. 2, we argued that one should not simply use the net growth function in the patch approximation, but rather split net growth into births and deaths. This issue arises in many other situations as well. In stochastic models, for example, births and deaths need to be treated differently. A simple linear Markov pure-birth process has zero probability of extinction, whereas a birth–death process with the same net growth rate has a positive extinction probability (Kot 2001). In structured models,

basic bookkeeping rules require that individuals are removed only from their current state (e.g. age, location, velocity) whereas offspring maybe placed into a different state from the parent.

In general, there are many ways to split a net growth function in the RDE into reproduction and death. When we compare the results of the RDE model with those of the corresponding MOT approximation, we have to choose how we partition the growth function in the RDE into the birth and death terms for the MOT approximation. Ideally, in empirical examples, the two processes can be measured separately so that no ambiguity exists. In our theoretical study, we can investigate this question in more detail by comparing different ways of partitioning net growth into births and deaths.

We begin with the linear model and the resulting critical patch size. The RDE model has the single parameter $r = b - m$. The MOT approximation depends on m and b separately. We begin by investigating how the relative difference between L_c and $\hat{L}_c$ depends on m, given that $b - m = r$ is constant. In other words: how much does it matter whether we include deaths into the movement or the population dynamics term?

To that end, we write the mortality as $m = m_1 + (m - m_1)$, where m_1 denotes the portion that will be applied to calculate $T(x)$ and $\overline{T}$, and $m - m_1$ the portion that will be included into the population dynamics. We denote $\overline{T}(m)$ as the expression in (28). Then the critical domain size of the MOT approximation is given by the root, $\hat{L}_c$, of the equation $\overline{T}(m_1)(b-(m-m_1)) = 1$. We ask how $\hat{L}_c$ depends on m_1. Specifically, when $m_1 = m$, we have the MOT approximation as calculated previously; when $m_1 = 0$, we have the MFPT approximation from Sect. 2.

For this comparison, we note that the MFPT with mixed boundary conditions from (25) is given by

$$T(x) = \frac{1}{2D}\left(-x^2 + xL + \frac{L}{\chi}\right), \quad \overline{T} = \frac{L^2}{12D}\left(1 + \frac{6}{L\chi}\right). \tag{33}$$

and the critical patch size for the MFPT approximation is given explicitly by

$$\hat{L}_c = -\frac{3}{\chi} + \sqrt{\frac{9}{\chi^2} + \frac{12D}{r}}. \tag{34}$$

When $m_1 > 0$, the critical patch size (29) for the MOT approximation cannot be given explicitly.

In Fig. 1, we plot L_c and $\hat{L}_c$ for different values of m_1 as a function of p (recall $\chi = \frac{p}{1-p}\sqrt{\frac{r}{D}}$). For small values of p, the approximation is particularly accurate, but even for $p \approx 1/2$ the relative difference is well below 5 %. We observe that for the chosen parameter values the MFPT approximation ($m_1 = 0$) is closer than its MOT counterpart ($m_1 > 0$).

We can look at the critical patch size condition $\overline{T}(m_1)(b - (m - m_1)) = 1$ as a function of m_1. Clearly, $\overline{T}(m)$ is a decreasing function. The slope of the function $\overline{T}(m_1)(r + m_1)$ is given by

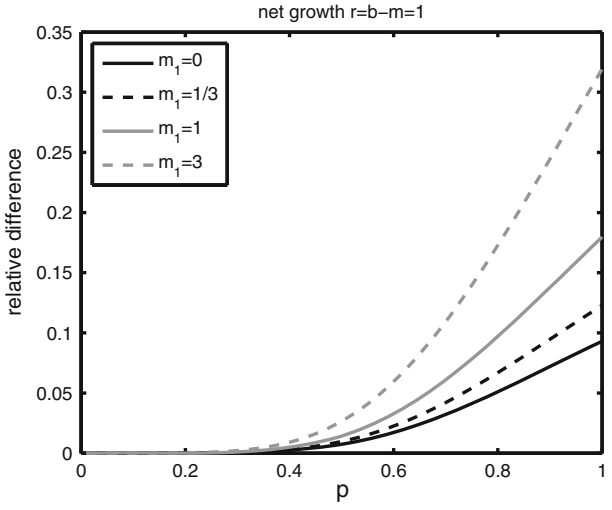

Fig. 1 The relative difference of the critical patch sizes $(\hat{L}_c - L_c)/\hat{L}_c$ increases as the probability of leaving the patch increases. L_c is as in (26) whereas $\hat{L}_c$ results from the implicit equation (29). The non-spatial approximation overestimates the spatially explicit value. The maximum relative difference is around 10 % when net growth consists of only births ($m_1 = 0$). When net growth is composed of births and deaths the maximum relative difference can increase to around 33 %. Parameters are $D = r = 1$

$$\frac{d}{dm_1}\overline{T}(m_1)(r+m_1) = \overline{T}'(m_1)(r+m_1) + \overline{T}(m_1). \tag{35}$$

The first term is negative, since occupancy time decreases with death rate; the second is positive. Hence, when r is small the slope is positive, at least for small m_1; when r is large the slope is negative, at least for large m_1. In the first case, the function is increasing, in the second it is decreasing. Numerically, we found that the function $\overline{T}(m_1)(r+m_1)$ can, in rare cases, have a local extremum for some intermediate value $0 < m_1 < r$, but most often is monotone in that interval. Since the MFPT approximation (already) overestimates L_c for the RDE, the MOT approximation exaggerates this overestimation when the function $\overline{T}(m_1)(r+m_1)$ is decreasing.

Next, we consider the spatial profile of the steady state. The explicit expression for its profile follows from (8) and (9), as

$$u^*(x) = \frac{\overline{T}(b-(m-m_1))-1}{\overline{T}\alpha(\overline{T}(m-m_1)+1)}T(x) \tag{36}$$

with $T(x)$ given by (27) for $m_1 > 0$ and by (33) in the MFPT case.

Figure 2a demonstrates that the approximation is very close to the RDE result for relatively small domains and a wide range of p values. The shape of the steady profile changes as the partitioning of net growth rate between birth and death is changed. This effect is best seen on large domains (Fig. 2b). On a large domain the steady state profile approaches the value of the spatially homogeneous non-trivial steady state everywhere in the domain except in a region close to the boundary. With net growth

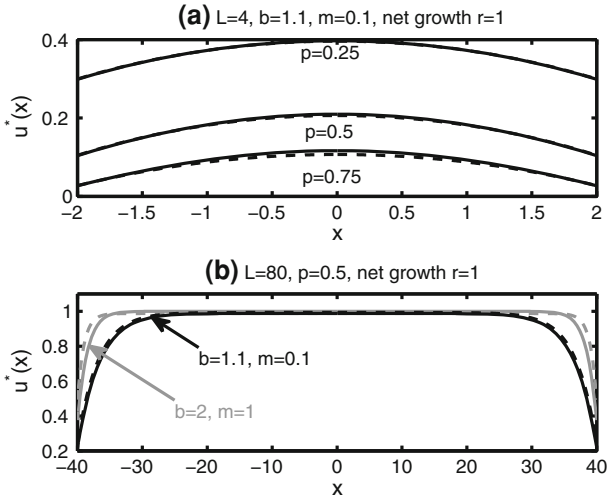

Fig. 2 The steady state profile $u^*(x)$ of (24) (*solid line*) is well described by the MOT approximation from Eq. (30) with $m_1 = m$ (*dashed line*). **a** On a small domain the approximation loses accuracy as p increases and the boundary conditions approach those of a completely hostile boundary. **b** Fixing the net growth rate $r = b - m$, increased mortality reduces the size of the region affected by loss through the boundary. Parameters: $D = 1$, maximum population density scaled to 1

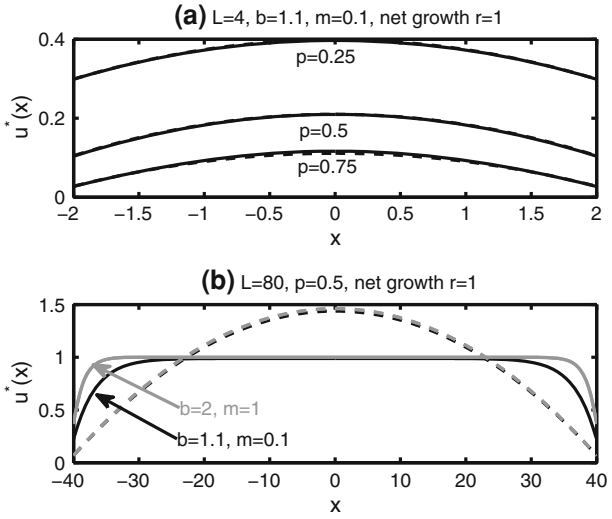

Fig. 3 The steady state profile $u^*(x)$ of Eqs. (24, 25) (*solid line*) is well described by the MFPT approximation (36) with $m_1 = 0$ (*dashed line*) on a small domain (**a**). On a large domain, MFPT is unable to accurately capture the shape of the steady state profile. Parameters: $D = 1$, maximum population density scaled to 1

$(b - m)$ fixed, increasing m reduces the size of this boundary region. To understand this observation, we consider the eigenvalue $((m - b)m/b)$ corresponding to spatially homogeneous steady state. The magnitude of the eigenvalue increases with the ratio

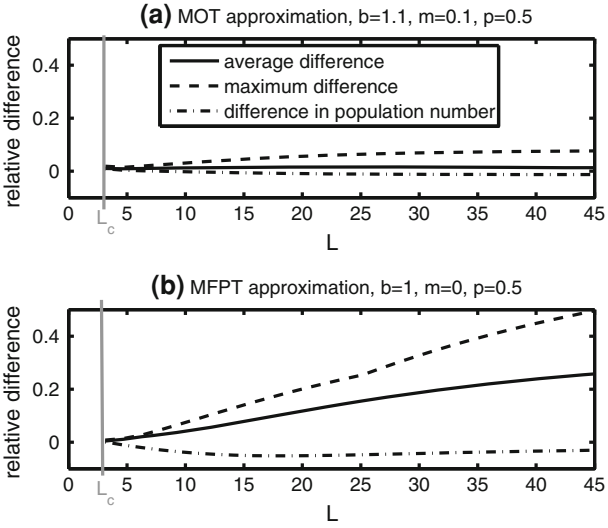

Fig. 4 Comparing the MOT with $m_1 = m$ (**a**) and MFPT (**b**) approximations of the steady state profile (36) to the numerical solution of the RDE (24, 25). We calculate the relative error in average and maximum difference as well as total population density between the RDE and the approximations. MOT has a relative error of less than 10 %. For large domains, MFPT has large error, unable to capture the shape of the profile. However, both approximations come within 5 % of the total number of individuals in the patch, and both consistently underestimate the value. Parameters: $D = 1$, maximum population density scaled to 1

m/b, thus as m increases the spatially homogeneous steady state is reached more rapidly, and movement at the boundary will have only a localised effect.

The corresponding plots for the MFPT approximation in Fig. 3 reveal that the difference between the two approaches is small on small domains, but essential on larger domains. It is clear from the quadratic expression for $T(x)$ in (33) that $T(0)$ will grow as L grows whereas the steady state of the RDE and $T(0)$ from (11) remain bounded. In particular, the MFPT approximation cannot capture the plateau that forms at the carrying capacity at the center of the domain.

When considering other metrics for the comparison between the steady state of the RDE and the two approximations, we see that the number of individuals in a patch is predicted fairly accurately by both approximations. But when we look at the maximum and average relative difference between the approximations and the actual steady state profile across the patch, then MOT does much better than MFPT (Fig. 4).

4.3 Single patch with a non-hostile exterior

The assumption of hostile exterior rarely applies to terrestrial landscapes. In fact, several studies showed the importance of even low-quality ‘matrix’ around and between high quality patches (Ludwig et al. 1979; Artiles et al. 2008). Following the approach by Ludwig et al. (1979), we include the exterior of the patch into the boundary conditions and thereby reduce the problem to the same kind as in the previous section.

The linearized model for the dynamics of a population at low density on the focal patch and the exterior is

$$\begin{aligned} \frac{\partial u}{\partial t} &= D_1 \frac{\partial^2 u}{\partial x^2} + (b_1 - m_1)u, \qquad x \in (-l, l), \\ \frac{\partial u}{\partial t} &= D_2 \frac{\partial^2 u}{\partial x^2} - m_2 u, \qquad\quad x \notin [-l, l], \end{aligned} \tag{37}$$

where $D_1(D_2)$ is the diffusion coefficient inside (outside) the focal patch, b_1 is the maximum birth rate inside the focal patch, and m_1 (m_2) is the death rate inside (outside) the focal patch. The limit $m_2 \to \infty$ corresponds to hostile surroundings.

Individuals who leave the focal patch enter the surroundings and vice versa. Mathematically, the population flux should be continuous at the interfaces $x = \pm l$ (Ludwig et al. 1979). Population density will typically be discontinuous across an interface if movement behavior of individuals differs in the two adjacent habitat types; depending on movement assumptions, Ovaskainen and Cornell (2003) derived different possible conditions, namely

$$\begin{aligned} &\textbf{(I)}\ \sqrt{D_1}u(-l^+, t) = \sqrt{D_2}u(-l^-, t) \ \text{ and } \ \sqrt{D_1}u(l^-, t) = \sqrt{D_2}u(l^+, t), \\ &\textbf{(II)}\ D_1 u(-l^+, t) = D_2 u(-l^-, t) \ \text{ and } \ D_1 u(l^-, t) = D_2 u(l^+, t). \end{aligned} \tag{38}$$

Here, superscripts $^{\pm}$ stand for the limits from the right and left, respectively. Condition (**I**) results from the assumption that step sizes in the focal patch and surroundings differ but movement rates are identical. Condition (**II**) results from the opposite assumption; step sizes are identical but movement rates differ between patch and surroundings. For a detailed discussion of how these interface conditions affect population dynamics in a variety of models, see Maciel and Lutscher (2013).

Following Ludwig et al. (1979), the persistence problem and the steady-state equations for (37) are equivalent to considering the equation on the focal patch alone, but with mixed boundary conditions

$$u_x(-l, t) = \chi u(-l, t), \quad u_x(l, t) = -\chi u(l, t), \tag{39}$$

where the two interface matching conditions translate into

$$\textbf{(I)}\ \chi = \sqrt{m_2/D_1} \ \text{ or } \textbf{(II)} \ \ \chi = \sqrt{m_2/D_2} \tag{40}$$

Since the problem formulation is now the same as in the previous section, the MOT and critical patch size are given by (27) and (29), respectively.

Critical patch size increases as the quality of the patch exterior decreases. The occupancy time approximation is able to capture the distinction between the critical patch sizes obtained under the two types of interface matching conditions (Fig. 5) and is within 10 % of L_c. As in Sect. 4.3, the MOT approximation performs best when $m_1 = 0$. When $\sqrt{m_2/D_2}$ is small, individuals move rapidly in the exterior and so have an increased probability of returning to the focal patch. This is equivalent to small p in

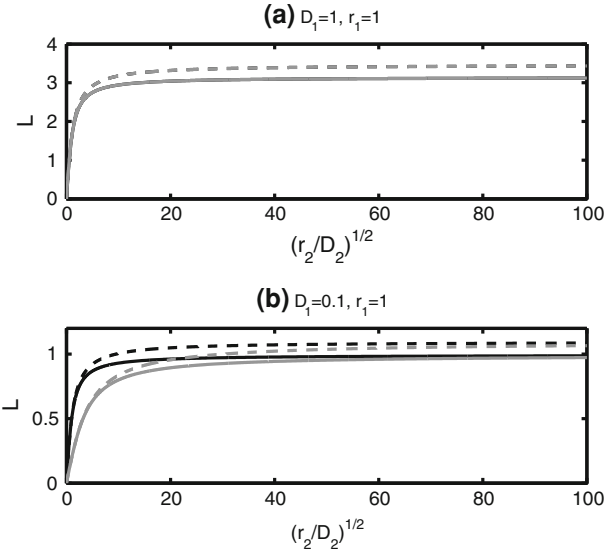

Fig. 5 Critical patch size increases with the inverse of the movement rate in the patch exterior. In **a**, $D_1 = D_2$, so that the difference in boundary conditions (40) disappears. In **b**, $D_1 = 0.1$, $D_2 = 1$, and the results for the different boundary conditions differ. In all cases $\hat{L}_c$ (*dashed lines*) is within 10 % of L_c (*solid lines*). L_c is as in (26) and $\hat{L}_c$ is implicitly given by (29) with χ as in (40). Fixed parameters are $m_1 = 0$ and $r_1 = b_1 = 1$. *Darker lines* are for interface conditions (**I**), *lighter grey* is for interface conditions (**II**)

Fig. 1. In this scenario, the occupancy time approximation with $m_1 \neq 0$ also performs well.

4.4 Multiple patches: core and buffer

For our first example of a two-patch model, we consider a variant of the classical KISS model, first studied by Cantrell and Cosner (1999). Specifically, we divide the reserve into a 'core habitat' of size $2L_1$, where conditions are optimal, surrounded by a 'buffer zone' of width L_2, where conditions are less favorable but still better than hostile. In the limiting case $L_2 \to \infty$, we retrieve the situation from the previous section. At the outer boundary of the buffer zone, we impose hostile conditions; at the interface between the core and the buffer, we assume that individuals turn towards the core with probability p and towards the buffer with probability $(1 - p)$. The interface conditions are then a combination of the conditions in the previous two sections: the flux is continuous at the interface but the density has a discontinuity that depends on movement rates (as in (38)) *and* core habitat preference (as in (25)); see Appendix A for details. Cantrell and Cosner (1999) implemented habitat preference as discontinuous flux conditions at the interface; see Maciel and Lutscher (2013) for a discussion of these two different approaches.

To find the matrix $\mathcal{T}$ for the patch approximation, we calculate the average time that an individual, originally located in the core habitat, spends in the core and buffer, respectively, and the same for initial location in the buffer zone and obtain

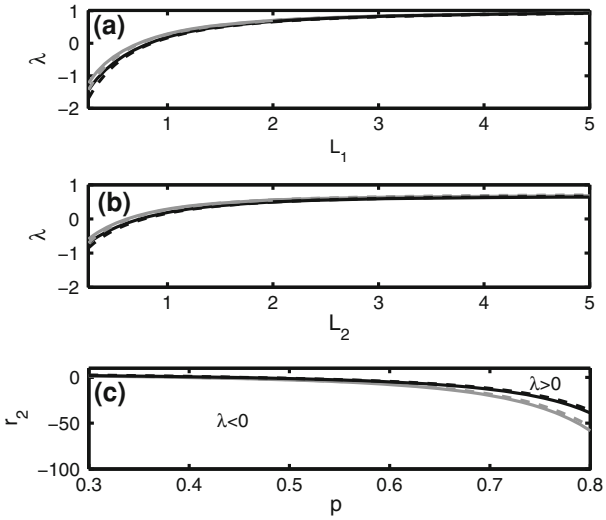

Fig. 6 Increasing the size of the core or buffer increases average populations growth rate, (**a**) and (**b**) respectively. The MOT approximation (*dashed line*) is virtually indistinguishable from the analytical solution of the RDE (*solid line*). *Black lines* correspond to interface conditions (**I**), *grey lines* correspond to (**II**); see Appendix A for details. In (**c**) critical patch size is plotted as a function of preference for the core. When $r_2 > 0$, we have chosen $m_2 = 0$ and $b_2 = r_2$. When $r_2 < 0$, then $m_2 = -r_2$ and $b_2 = 0$. In all plots $m_1 = 0$ and $b_1 = r_1$ and $D_1 = r_1 = L_1 = L_2 = 1$, $r_2 = 0.5$, and $D_2 = 1.5$, unless indicated otherwise

$$\mathcal{T} = \begin{bmatrix} \frac{L_1^2}{3D_1} + \frac{L_1 k}{\sqrt{m_2 D_2}} \tanh\left(L_2\sqrt{\frac{m_2}{D_2}}\right) & \frac{k}{m_2}\left(1 - \left[\cosh\left(L_2\sqrt{\frac{m_2}{D_2}}\right)\right]^{-1}\right) \\ \frac{L_1}{L_2 m_2}\left(1 - \left[\cosh\left(L_2\sqrt{\frac{m_2}{D_2}}\right)\right]^{-1}\right) & \frac{1}{m_2}\left(1 - \frac{1}{L_2}\sqrt{\frac{D_2}{m_2}} \tanh\left(L_2\sqrt{\frac{m_2}{D_2}}\right)\right) \end{bmatrix}, \quad (41)$$

detailed calculations are given in Appendix A. The determinant of this matrix is positive, the matrix $\mathbf{M} = -\mathcal{T}^{-1}$ has negative diagonal entries and positive off-diagonal entries.

In this example, we demonstrate that the MOT approximation not only estimates the persistence conditions, but the principal eigenvalue of the RDE (Fig. 6). Increasing the size of the buffer increases the average population growth rate, but as Cantrell and Cosner (1999) noted there is a strict limit to this beneficial effect. Specifically, the dominant eigenvalue remains bounded away from unity even for very large buffer zones, whereas $\lambda = 1$ would be the dominant eigenvalue for a large core patch. Finally, increasing the preference for the core ensures that even a very poor quality buffer ($r_2 < 0$) is beneficial (Fig. 6c).

4.5 Periodic landscape with two patch types

For a final example, we consider a periodic landscape of two patch types, alternating between favourable (of size L_1) and unfavourable (of size L_2) habitat as first studied by Shigesada et al. (1986). Within one period $[-L_2, L_1]$, we have the same linearized equations as with the core and buffer example (Sect. 4.4), namely

$$u_t = D_i u_{xx} - m_i u + b_i u, \quad x \in \Omega_i \tag{42}$$

with $r_i = b_i - m_i$, $\Omega_1 = [0, L_1]$ and $\Omega_2 = [-L_2, 0]$. The net growth rates satisfy $r_2 < 0 < r_1$. Periodicity allows us to reduce the problem to the domain $[-L_2/2, L_1/2]$ with with no-flux conditions

$$u_x(L_1/2, t) = 0, \quad u_x(-L_2/2, t) = 0. \tag{43}$$

The interface conditions at $x = 0$ are the same as the core and buffer examples: the flux of individuals is continuous at the interface, the density need not be; see (72).

To calculate the persistence conditions, we study the dominant eigenvalue of the matrix

$$-\mathcal{T}^{-1} + \begin{bmatrix} b_1 & 0 \\ 0 & b_2 \end{bmatrix} = \frac{1}{\det(\mathcal{T})} \begin{bmatrix} b_1 \det(\mathcal{T}) - T_{11} & T_{12} \\ T_{21} & b_2 \det(\mathcal{T}) - T_{22} \end{bmatrix}, \tag{44}$$

see Eqs. (22) and (23). The persistence boundary is given by the dominant eigenvalue of (44) being zero, i.e. the determinant of this matrix being zero. If we assume that the population experiences no death in favorable patches ($m_1 = 0$) and no growth in unfavorable patches ($b_2 = 0$), then this determinant has the particularly simple form

$$\frac{1 - b_1 T_{11}}{\det(\mathcal{T})}. \tag{45}$$

In particular, the persistence condition is $b_1 T_{11} = 1$. The MOT T_{11} can be calculated in the same way as for the previous example in Appendix A. Then one arrives at the explicit characterization of the persistence boundary as

$$\left(1 - \frac{L_1^2 r_1}{12 D_1}\right) \frac{2\sqrt{D_2 m_2}}{L_1 k r_1} = \left[\tanh\left(\sqrt{\frac{m_2}{D_2}} \frac{L_2}{2}\right)\right]^{-1}. \tag{46}$$

We note that since we are considering an infinite landscape, it is essential to include some mortality term into the movement operator to ensure that the MOT remains finite.

The persistence condition given by (46) is indistinguishable from that given by the full RDE (Fig. 7). The maximum size of the unfavourable patch that a species can tolerate increases as r_2 approaches zero (Fig. 7a). Similarly, the minimum size of the favourable patch that a species requires increases as the size of the unfavourable patch increases (Fig. 7b), and both types of interface condition predict the same trend. Maciel and Lutscher (2013) found that maximum unfavorable patch size increases with diffusivity D_2, and the interface conditions determined if this occurred in either a decelerating or accelerating fashion. The MOT approximation also successfully captures this distinction (Fig. 7c). The approximation performs well because we are estimating the spatially averaged eigenvalue of the RDE model, so this extra layer of averaging improves the approximation of the persistence condition by averaging out any errors in our approximation at the individual patch level. Moreover, the periodic

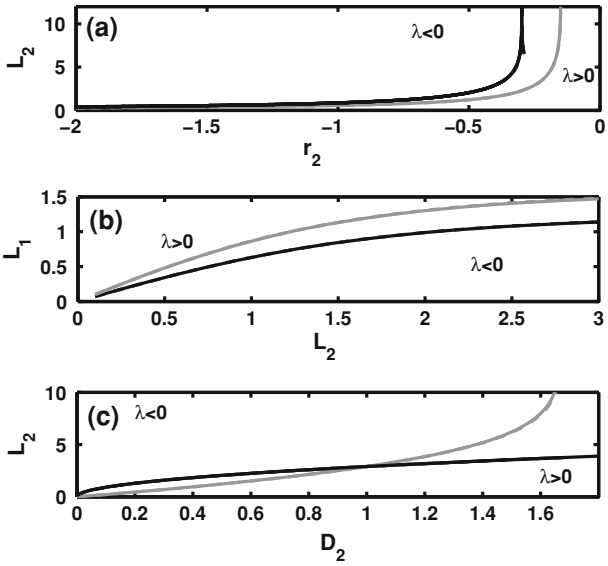

Fig. 7 In a periodic habitat, reducing the quality of or movement rate in unfavourable patches requires a reduction in the patch size to ensure persistence; see **a** and **c**. Larger favorable patches are needed for persistence as unfavorable patch size increases (**b**). The MOT approximation (46) (*dashed line*) is indistinguishable from the analytical solution of the RDE (42, 43) (*solid line*). The *black lines* correspond to interface conditions (**I**) and the *grey line* corresponds to (**II**). In all plots $m_1 = 0$, $b_1 = r_1 m_2 = -r_2$, $b_2 = 0$ and $D_1 = r_1 = L_1 = 1$, $r_2 = -0.5$, and $D_2 = 0.5$, unless indicated otherwise

habitat ensures there is no loss through dispersal, further enhancing the accuracy of the MOT approximation (compare to Fig. 1).

5 Derivation of the approximation results

In this section, we provide details of the formal calculations behind our approximations.

5.1 Single-patch approximation: steady state

The Green's function for $\mathcal{M}$ is defined by the equations

$$\begin{aligned} \frac{\partial G}{\partial t} &= \mathcal{M}(G, \mathbf{x}), \quad \text{in } \Omega \times (0, \infty), \quad \text{where } \Omega \subset \mathbb{R}^n \\ G(\mathbf{x}, 0) &= \delta(\mathbf{x} - \mathbf{y}), \quad \text{in } \Omega \\ \alpha(\mathbf{x}) \cdot \mathbf{J} &= G(\mathbf{x}, t) \quad \text{on } \partial\Omega \times (0, \infty). \end{aligned} \tag{47}$$

Since we assumed that individuals either leave the domain or die eventually, the dominant eigenvalue of $\mathcal{M}$ is negative, and the Green's function decays exponentially to zero.

Using the Green's function, we can write the solution of the nonlinear reaction–diffusion model (14) in integral form as

$$u(\mathbf{x},t) = \int_{\Omega} G(\mathbf{x},\mathbf{y},t)u_0(\mathbf{y})\,d\mathbf{y} + \int_0^t \int_{\Omega} G(\mathbf{x},\mathbf{y},t-s)\mathcal{F}(u(\mathbf{y},s),\mathbf{y})\,d\mathbf{y}ds. \quad (48)$$

Since the steady state $u^*(x)$ is independent of time, we may take the limit for large times

$$u^*(\mathbf{x}) = \lim_{t\to\infty}\left[\int_{\Omega} G(\mathbf{x},\mathbf{y},t)u_0(\mathbf{y})d\mathbf{y} + \int_0^t \int_{\Omega} G(\mathbf{x},\mathbf{y},t-s)\mathcal{F}(u^*(\mathbf{y}))d\mathbf{y}ds\right]. \quad (49)$$

By the properties of the Green's function, the first term on the right hand side will vanish. Taylor expanding $\mathcal{F}(u^*(\mathbf{x}))$ about the spatial average, $\bar{u}^*$, of $u^*(\mathbf{x})$ gives

$$u^*(\mathbf{x}) = \int_{\Omega} \int_0^{\infty} G(\mathbf{x},\mathbf{y},s)\left[\mathcal{F}(\bar{u}^*) + \mathcal{F}'(\bar{u}^*)(u^*(\mathbf{y}) - \bar{u}^*) + \text{h.o.t.}\right] d\mathbf{y}ds. \quad (50)$$

Now, we assume that $|u^*(\mathbf{x}) - \bar{u}^*|$ is small. Then we are left with the approximation

$$u^*(\mathbf{x}) \approx \mathcal{F}(\bar{u}^*) \int_0^{\infty} \int_{\Omega} G(\mathbf{x},\mathbf{y},s)\,d\mathbf{y}\,ds \quad (51)$$

If the movement operator is self-adjoint then the corresponding Green's function is symmetric, i.e. $G(\mathbf{x},\mathbf{y},s) = G(\mathbf{y},\mathbf{x},s)$. In this case, by (16), we have

$$u^*(\mathbf{x}) \approx \mathcal{F}(\bar{u}^*)T(\mathbf{x}), \quad (52)$$

and we have an approximation to the steady state profile of (14). Whether or not G is symmetric, we can average Eq. (51) and get

$$\bar{u}^* \approx \mathcal{F}(\bar{u}^*)\frac{1}{|\Omega|}\int_0^{\infty}\int_{\Omega}\int_{\Omega} G(\mathbf{x},\mathbf{y},s)d\mathbf{x}d\mathbf{y}ds = \mathcal{F}(\bar{u}^*)\bar{T}. \quad (53)$$

5.2 Single-patch approximation: eigenvalue

The dominant eigenvalue $-\lambda$ and corresponding positive eigenfunction ϕ of $\mathcal{M}$ in (47) satisfy the equation

$$\phi(\mathbf{x})e^{-\lambda t} = \int_{\Omega} G(\mathbf{x},\mathbf{y},t)\phi(\mathbf{y})\,d\mathbf{y}. \quad (54)$$

Now, we write $\phi(\mathbf{x}) = \bar{\phi} + \phi(\mathbf{x}) - \bar{\phi}$, where $\bar{\phi}$ is the spatial average of ϕ over Ω. Integrating Eq. (54) over the domain, we obtain

$$\bar{\phi}e^{-\lambda t} = \frac{\bar{\phi}}{|\Omega|}\int_\Omega\int_\Omega G(\mathbf{x},\mathbf{y},t)\,d\mathbf{y}\,d\mathbf{x} + \frac{1}{|\Omega|}\int_\Omega\int_\Omega G(\mathbf{x},\mathbf{y},t)(\phi(\mathbf{y})-\bar{\phi})\,d\mathbf{y}\,d\mathbf{x}. \tag{55}$$

Assuming that $|\phi(\mathbf{y})-\bar{\phi}|$ is small, integrating both sides with respect to t and applying the definition of $\bar{T}$ in (16), we obtain the desired approximation for the eigenvalue of the operator $\mathcal{M}$ as

$$\frac{1}{\lambda} \approx \frac{1}{|\Omega|}\int_0^\infty\int_\Omega\int_\Omega G(\mathbf{x},\mathbf{y},t)\,d\mathbf{x}\,d\mathbf{y}\,dt = \frac{1}{|\Omega|}\int_\Omega T(\mathbf{y})d\mathbf{y} = \bar{T}. \tag{56}$$

Matkowsky and Schuss (1977) obtained the same relationship under the alternative assumption that the diffusion coefficient in the movement operator $\mathcal{M}(u,\mathbf{x}) = \nabla\cdot(D(\mathbf{x})\nabla u))$ is small.

The approximation of the dominant eigenvalue leads to a population persistence condition in the case where the per capita fecundity function is a non-increasing function so that the population does not exhibit an Allee effect. Then the persistence condition for the reaction–diffusion equation (14) is obtained when the dominant eigenvalue of the linearized equation

$$\frac{\partial u}{\partial t} = \mathcal{M}(u,\mathbf{x}) + \tfrac{\partial\mathcal{F}}{\partial u}(0,\mathbf{x})u \tag{57}$$

is zero. Since the patch is assumed homogeneous, we have $\mathcal{F}(u,\mathbf{x}) = \mathcal{F}(u)$. Hence, with $\frac{\partial\mathcal{F}}{\partial u}(0) = r$, we find that the dominant eigenvalue of (57) is given by $-\lambda + r \approx -1/\bar{T} + r$, which is exactly the linearization of the MOT approximation (21) at zero.

Stability of a positive steady state in the spatially explicit equation is determined by the dominant eigenvalue μ of the operator $\mathcal{M} + \partial_u\mathcal{F}(u^*)$, i.e.

$$\mu\phi(\mathbf{x}) = \mathcal{M}(\phi,\mathbf{x}) + \frac{\partial\mathcal{F}}{\partial u}(u^*(\mathbf{x}),\mathbf{x})\phi(\mathbf{x}). \tag{58}$$

Assuming, again, that the patch is homogeneous within, and using the steady state approximation above, we write

$$\frac{\partial\mathcal{F}}{\partial u}(u^*(\mathbf{x})) = \frac{\partial\mathcal{F}}{\partial u}(\bar{u}^*) + \frac{\partial^2\mathcal{F}}{\partial u^2}(\bar{u}^*)(u^*(\mathbf{x})-\bar{u}^*) + \text{h.o.t.} \tag{59}$$

Keeping only the first term, we have an eigenvalue problem of the same form as (57), so that the stability boundary is given when

$$0 = \mu = -\lambda + \mathcal{F}'(\bar{u}^*) \approx -1/\bar{T} + \mathcal{F}'(\bar{u}^*) = 0, \tag{60}$$

which is the stability boundary for the MFPT approximation (21).

5.3 Multi-patch approximation

The derivation of the spatially implicit approximation in the multi-patch case is very similar to the steady state derivation in the single-patch case, the difference being that we average on each individual patch rather than over the entire domain. The spatially implicit model (15) and its steady state equation read

$$\dot{\mathbf{U}} = \mathbf{M}\mathbf{U} + \mathbf{F}(\mathbf{U}), \qquad \mathbf{U}^* = -\mathbf{M}^{-1}\mathbf{F}(\mathbf{U}). \tag{61}$$

The steady state solution for the spatially explicit equation satisfies

$$u^*(\mathbf{x}) = \int_0^\infty \int_\Omega G(\mathbf{x}, \mathbf{y}, s)\mathcal{F}(u^*(\mathbf{y}))d\mathbf{y}ds. \tag{62}$$

Now we take averages over each of the patches that make up the habitat, i.e.

$$\bar{u}_j^* = \frac{1}{|\Omega_j|}\int_{\Omega_j} u^*(\mathbf{x})d\mathbf{x}, \tag{63}$$

and use Taylor expansion on each patch to arrive at

$$u^*(\mathbf{x}) = \sum_j \int_0^\infty \int_{\Omega_j} G(\mathbf{x}, \mathbf{y}, s)\left[\mathcal{F}_j(\bar{u}_j^*) + \mathcal{F}_j'(\bar{u}_j^*)(u^*(\mathbf{x}) - \bar{u}_j^*) + \text{h.o.t}\right]d\mathbf{y}ds. \tag{64}$$

Averaging this equation over patch i and assuming that $|u^*(\mathbf{x}) - \bar{u}_j^*|$ is small, we obtain

$$\bar{u}_i^* = \frac{1}{|\Omega_i|}\sum_j \int_0^\infty \int_{\Omega_i}\int_{\Omega_j} G(\mathbf{x}, \mathbf{y}, s)d\mathbf{y}d\mathbf{x}ds\ \mathcal{F}_j(\bar{u}_j^*). \tag{65}$$

We can conveniently write this equality in matrix-vector notation as

$$\mathbf{u}^* = \mathcal{T}\mathbf{F}(\mathbf{u}^*), \quad \mathbf{u}^* = (\bar{u}_1^*, \ldots, \bar{u}_n^*)' \tag{66}$$

where $\mathbf{F}(\mathbf{u}) = (\mathcal{F}_1(u_1), \ldots, \mathcal{F}_n(u_n))'$ and matrix $\mathcal{T} = (T_{ij})$ has the entries

$$\begin{aligned} T_{ij} =& \frac{|\Omega_j|}{|\Omega_i|} \frac{1}{|\Omega_j|} \int_{\Omega_j} \int_{\Omega_i} \int_0^\infty G(\mathbf{x}, \mathbf{y}, s)\, ds d\mathbf{x} d\mathbf{y} \\ =& \frac{|\Omega_j|}{|\Omega_i|} \frac{1}{|\Omega_j|} \int_{\Omega_j} \int_{\Omega_i} B(\mathbf{x}, \mathbf{y})\, d\mathbf{x} d\mathbf{y} \\ =& \frac{|\Omega_j|}{|\Omega_i|} \frac{1}{|\Omega_j|} \int_{\Omega_j} T_{\Omega_i}(\mathbf{y})\, d\mathbf{y}. \end{aligned} \tag{67}$$

Hence, we choose $-\mathbf{M}^{-1} = \mathcal{T}$, so that the steady state equation for the spatial averages of the spatially explicit model is to lowest order the same as for the patch model

$$\dot{\mathbf{U}} = -\mathcal{T}^{-1}\mathbf{U} + \mathbf{F}(\mathbf{U}). \tag{68}$$

Combining the argument for eigenvalue approximation in the single-patch case with the patch-averaging idea above shows that the dominant eigenvalue of the movement operator approximately satisfies the equation

$$\frac{1}{\lambda}\Phi = \mathcal{T}\Phi, \tag{69}$$

so that the persistence condition of the spatially explicit equation and the patch equation are approximately the same.

6 Discussion

Habitat fragmentation and its impact on population persistence is of key concern to landscape ecologists and conservationists. Diffusion models have been extensively used by theoreticians to determine critical thresholds for extinction (Cantrell and Cosner 2003). This mechanistic framework provides a powerful tool for integrating complex descriptions of individual movement behavior into a model of a temporally changing population distribution; see Turchin (1998) and references therein.

To study persistence in a heterogeneous landscape over a large spatial scale, the habitat is often modelled as a system of coupled patches, giving rise to ordinary differential equation models. This approach circumvents the problems of analyzing, parameterizing and simulating highly complex RDE models at this scale. Cantrell et al. (2012) discuss and compare the two different approaches in a simple landscape consisting of five patches. The immigration and emigration rates of these patch models are first-order decay processes, often determined by phenomenological arguments, for example in the metapopulation literature (Hanski and Ovaskainen 2000). More recently, such rates have been approximated using the eigenvalue of the corresponding RDE model (Strohm and Tyson 2012; Vasilyeva and Lutscher 2012), see also page

130 in Cantrell and Cosner (2003), or by simple approximations of the flux at patch boundaries (Wakano et al. 2011; Weins et al. 1993; Cantrell et al. 2012).

Our approach is to derive immigration and emigration rates from occupancy times for the movement equations. It turns out that the dominant eigenvalues of the resulting patch models approximate those of the RDE, thereby retaining as much information about the complex movement and landscape heterogeneity as possible. The advantage of this approach is that transfer rates between patches include information about the habitat crossed in between patches as well as properties of the patches themselves, relating to shape, size and boundaries. The impact of these patch characteristics are not visible in the one-dimensional setting but do appear in two dimensions since the Greens function depends on these characteristics and the mean occupancy time is obtained by integrating the Greens function over the patch, see Eq. (16). We illustrate this dependence in Appendix B where we demonstrate that mean occupancy time depends nonlinearly on the dimensions of a rectangular domain of fixed area. Computing MOT for more complex domains of two or more spatial dimensions requires numerically solving a system of elliptic PDEs to find MOT. However, this computation needs to be carried out only once to obtain the movement rates between patches for the corresponding ODE system. Therefore, our approach could still be computationally simpler than solving the reaction–diffusion equation on a large complex heterogeneous domain as McKenzie et al. (2009) found in their application of MFPT to study functional responses.

In the case of a single patch we demonstrated that the rate of leaving is the inverse of the spatially averaged mean occupancy time for this patch. Mean occupancy time is the expected time an individual is in the patch and alive. It can be measured directly using mark recapture techniques (Frair et al. 2005) or can be derived from a mechanistic description of movement that is typically used in the derivation of the corresponding RDE models (Ovaskainen and Cornell 2003; McKenzie 2006). Mean occupancy time satisfies an elliptic equation involving the adjoint of the movement operator as discussed in Sect. 3, and it is this relationship to the corresponding PDE model that ensures the eigenvalues of the patch model correspond to those of the RDE.

Our approach is the continuous-time analogue of the average dispersal success approximation, used to approximate integrodifference equation models of discrete time continuous space processes by discrete time patch models (Van Kirk and Lewis 1997; Lutscher and Lewis 2004). Average dispersal success is the spatially averaged probability of starting in the patch and staying there, which is related to the mean occupancy time, essentially the average time spent in the patch. Both these quantities are spatial integrals of the Green's functions of the associated movement operators. Consequently, as with dispersal success approximations, we demonstrated that we can also approximate the spatial distribution of the population within a patch. This is a refinement on the residence index presented by Turchin (1998). The average dispersal success approximation has already proved to be a useful practical tool for ecologists (Cobbold et al. 2005), particularly in determining critical reserve sizes (Fagan and Lutscher 2006). We hope that the mean occupancy time approximation will afford the same benefits to continuous time problems.

Our MOT approximation relies on the assumption that $|u^*(x) - \bar{u}^*|$ is small, meaning that the steady state is close to the spatial average. A similar assumption is made

in the development of the average dispersal success approximation (Van Kirk and Lewis 1997). For a large domain, density $u^*(x)$ is indeed close to $\bar{u}^*$, as illustrated in Fig. 2, and only in a very small region near the boundary does this assumption fail. For smaller domains where the boundary region affects a larger portion of the domain an argument analogous to that proposed by Van Kirk and Lewis (1997) applies. Near the boundary, occupancy time density (17) is small as there is a high probability of exiting the domain here, and this fact ensures the product $\int^\infty G(\mathbf{x}, \mathbf{y}, s)(u^*(\mathbf{y}) - \bar{u}^*)\, ds$ in our approximation (50) is small even when $|u^*(x) - \bar{u}^*|$ is not. In the centre of such a domain $|u^*(x) - \bar{u}^*|$ will be small as loss through the boundary is low and has a small effect on the domain interior. As we saw in Fig. 2 our approximation begins to fail when we apply mixed boundary conditions with a high probability, p, of leaving the domain, which in turn leads to a larger effect of the boundary on the domain interior and so our approximation underestimates the steady state distribution in this case. Nonetheless our approximation works surprisingly well, even in cases where one might expect it to fail.

We are unaware of previous applications of mean occupancy time in mathematical biology, but mean first passage time has been used in mathematical ecology before to study encounter rates between predator and prey (McKenzie 2006), and extensively in chemistry and physics (Hanggi et al. 1990). In those cases, death during movement is ignored. Mean first passage time has been used to approximate reaction rates based on heuristic arguments. We believe our work is the first attempt to give this relationship a more formal grounding. In all cases, however, there is the underlying implicit assumption that occupancy times are exponentially distributed. While this is not generally the case, the reaction rate approximation is very robust to the relaxation of this assumption (Kolpas and Nisbet 2010).

The importance of including mortality in the movement operator, used to derive mean occupancy time, was clearly demonstrated in Sect. 4. Accuracy of our approximations is affected by whether individuals die in their current location. Why this is so important is to some extent an open question although similar issues arise in partitioning births and deaths in reaction–transport equations (Hadeler 2000) and in stochastic models of birth–death processes (Samia and Lutscher 2012).

In Sect. 4, we compared the persistence conditions derived from our patch models to the analogous results for the RDE counterparts. Typically, the approximation is within 10 % and in many cases indistinguishable from the analytic result of the RDE. The power of this approximation is also highlighted by its flexibility to include effects of the habitat in which the patches are located. The framework can be also readily generalised to a stochastic framework. While studying stochastic RDEs is incredibly demanding, investigating a spatially implicit reduction using MOT is feasible. In the same spirit, Samia and Lutscher (2012) used the dominant eigenvalue of the movement operator to obtain a spatially implicit formulation of a stochastic model for persistence in a river.

As our approach is derived from a general movement operator it is flexible, allowing us to include bias in movement at patch boundaries for example. Such bias is important for issues of habitat preference. Habitat preference is is not classically included in patch models although Hanski and Ovaskainen (2000) offer a framework for doing this in

the context of metapopulations, but do not prescribe the relation between migration rates and behaviour explicitly.

Beyond this initial development of our theory for mean occupancy time patch models there are a number of future challenges. An important consideration is the incorporation of non-linear death rates into our approach. While they can readily be included as part of the net reproduction function $f(u)$, it is not clear that this is necessarily the correct approach given the importance of including linear death rates with the movement operator. Non-linear death rates naturally emerge in models of interacting populations, and this is then the major challenge to extending our theory to such systems. The eigenvalue approximations by Strohm and Tyson (2012); Vasilyeva and Lutscher (2012) consider all death terms as part of the net reproduction function with great success. The same is true for the corresponding theory for integrodifference equations (Lutscher and Lewis 2004).

In addition to the ecological examples we have discussed in this work, the theory is also readily applicable to other contexts where a spatially patchy environment naturally arises. One such setting is to describe the distribution of proteins or chemicals among cellular compartments (patches) within a cell. Diffusion models are pervasive throughout the mathematical biology literature, and increasing attention is being placed on studying such models in a heterogeneous environment. Our framework offers an approach to simplify this analysis while faithfully capturing the properties of the complex RDE models they approximate.

Acknowledgments Some of this work was carried out while the first author visited Ottawa, funded by the Carnegie Trust for the Universities of Scotland. Additional support came from a grant to FL by the Canadian research network MITACS. FL is partially funded by a Discovery Grant from the Natural Sciences and Engineering Research Council of Canada.

Appendix A: Core and buffer habitat

We consider a core habitat, say a reserve, of length $2L_1$, with a buffer zone of length L_2 attached to the core on either side (Cantrell and Cosner 1999). Since the one-dimensional model is symmetric with respect to the middle of the core habitat, we use this symmetry to reduce the model to the core ($\Omega_1 = [0, L_1]$) and the buffer ($\Omega_2 = [-L_2, 0]$). The linearized equations for the density of individuals in the core and buffer are

$$u_t = D_i u_{xx} - m_i u + b_i u, \quad x \in \Omega_i \tag{70}$$

with $r_i = b_i - m_i$ and $r_1 > r_2$. We have a hostile boundary at $x = -L_2$ and, due to symmetry, no-flux conditions at $x = L_1$, i.e.

$$u_x(L_1, t) = 0, \quad u(-L_2, t) = 0. \tag{71}$$

At the interface between core and buffer, we require the flux to be continuous, but the density can be discontinuous if either there is movement preference by the

individuals or if the diffusion rates differ between core and buffer (Ovaskainen and Cornell 2003), i.e.

$$D_1 u_x(0^+,t) = D_2 u_x(0^-,t), \quad u(0^+,t) = k u(0^-,t), \tag{72}$$

where superscripts $\pm$ stand for right- and left-sided limits. Parameter k summarizes bias and changes in movement. If individuals prefer the core habitat with probability p, then either (**I**) $k = \frac{p\sqrt{D_2}}{(1-p)\sqrt{D_1}}$ or (**II**) $k = \frac{pD_2}{(1-p)D_1}$, see (38).

We denote $\mathcal{M}$ as the operator defined by (70–72) with $b_1 = b_2 = 0$. To determine the adjoint operator, we use the definition

$$\int_{-L_2}^{L_1} v(x)\mathcal{M}u(\cdot)dx = \int_{-L_2}^{L_1} u(x)\mathcal{M}^* v(\cdot)dx \tag{73}$$

We find that $\mathcal{M}^*$ is given by $D_i v_{xx} - m_i v$ for $x \in \Omega_i$ with interface and boundary conditions,

$$k D_1 v_x(0^+,t) = D_2 v_x(0^-,t), \quad v(0^+,t) = v(0^-,t), \tag{74}$$

$$v_x(L_1,t) = 0, \quad v(-L_2,t) = 0. \tag{75}$$

Occupancy time in the core (T_{Ω_1}) and buffer (T_{Ω_2}) satisfy (20), which yields the following ODEs

$$D_1 \frac{d^2 T_{\Omega_1}}{dy^2} - m_1 T_{\Omega_1} = -1, \quad y \in \Omega_1; \quad D_2 \frac{d^2 T_{\Omega_1}}{dy^2} - m_2 T_{\Omega_1} = 0, \quad y \in \Omega_2; \tag{76}$$

$$D_1 \frac{d^2 T_{\Omega_2}}{dy^2} - m_1 T_{\Omega_2} = 0, \quad y \in \Omega_1; \quad D_2 \frac{d^2 T_{\Omega_2}}{dy^2} - m_2 T_{\Omega_2} = -1, \quad y \in \Omega_2. \tag{77}$$

Setting $m_1 = 0$, and using the boundary condition at $x = L_1$, we obtain

$$T_{\Omega_1}(y) = \frac{1}{D_1}\left(-\frac{y^2}{2} + L_1 y + C\right), \quad y \in \Omega_1. \tag{78}$$

A convenient representation of the solution on Ω_2 that takes the boundary at $x = -L_2$ into account, is

$$T_{\Omega_1}(y) = A \sinh\left(\sqrt{\frac{m_2}{D_2}}(y + L_2)\right), \quad y \in \Omega_2. \tag{79}$$

The interface condition for T_{Ω_1} gives

$$C = D_1 A \sinh\left(\sqrt{\frac{m_2}{D_2}} L_2\right), \tag{80}$$

whereas the condition on T'_{Ω_1} gives

$$A = \frac{kL_1}{\sqrt{D_2 m_2}\cosh\left(\sqrt{\frac{m_2}{D_2}}L_2\right)}. \tag{81}$$

The calculations for T_{Ω_2} are similar.

The definitions in (23) now give the elements of the matrix $\mathcal{T}$. Finally, the average population growth rate is given by the eigenvalues of the matrix

$$\begin{bmatrix} b_1 & 0 \\ 0 & b_2 \end{bmatrix} - \mathcal{T}^{-1}. \tag{82}$$

Appendix B: MFPT of a rectangle

We consider the rectangular domain $\Omega = [0, a] \times [0, b]$ and the diffusion equation

$$\frac{\partial u}{\partial t} = D\left(\frac{\partial^2 u}{\partial x^2} + \frac{\partial^2 u}{\partial y^2}\right), \quad (x, y) \in \Omega \tag{83}$$

with hostile boundary conditions $u = 0$ for $x \in \{0, a\}$ and $y \in \{0, b\}$.

The dominant eigenvalue can be calculated by standard separation of variables as

$$\lambda = -\pi^2 D\frac{a^2 + b^2}{a^2 b^2}. \tag{84}$$

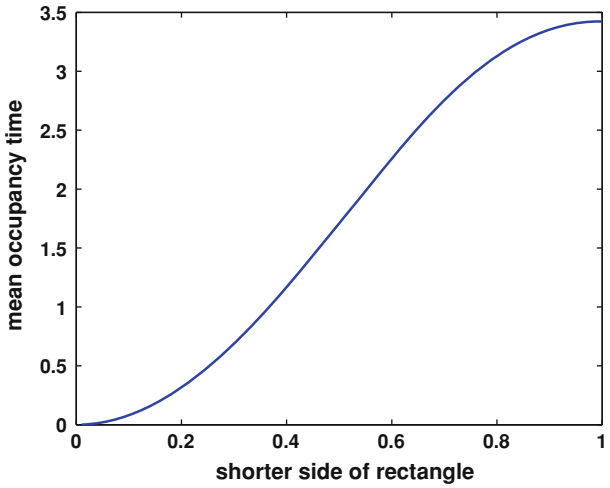

Fig. 8 Plot of MOT equation (89) for a rectangular domain with hostile boundary conditions. The area is fixed to 1, while the dimensions of the domain are varied, so illustrate how shape can effect MOT. The parameter $D = 1$

When we keep the area of the rectangle constant, we set $b = 1/a$. In that case, the dominant eigenvalue is maximal when $a = 1$.

The MFPT is given by the equation

$$D\left(\frac{\partial^2 T}{\partial x^2} + \frac{\partial^2 T}{\partial y^2}\right) = -1 \quad \text{on} \quad \Omega. \tag{85}$$

The ansatz

$$T(x, y) = \sum_{m,n} B_{m,n} \sin\left(\frac{m\pi x}{a}\right) \sin\left(\frac{n\pi x}{b}\right) \tag{86}$$

leads to the condition

$$\sum_{m,n} \hat{B}_{m,n} \sin\left(\frac{m\pi x}{a}\right) \sin\left(\frac{n\pi x}{b}\right) = 1, \quad \hat{B}_{m,n} = D\pi^2 B_{m,n}\left(\frac{m^2}{a^2} + \frac{n^2}{b^2}\right). \tag{87}$$

The coefficients must satisfy $\hat{B}_{m,n} = 16/(nm\pi^2)$ when n and m are odd and $\hat{B}_{m,n} = 0$ otherwise. Accordingly, we obtain

$$T(x, y) = \sum_{m,n \text{ odd}} \frac{16}{nmD\pi^2}\left(\frac{m^2}{a^2} + \frac{n^2}{b^2}\right)^{-1} \sin\left(\frac{m\pi x}{a}\right) \sin\left(\frac{n\pi x}{b}\right). \tag{88}$$

After integrating, we find

$$\overline{T} = \sum_{m,n \text{ odd}} \frac{16}{nmD\pi^2} \frac{a^2 b^2}{a^2 n^2 + b^2 m^2}. \tag{89}$$

We evaluate this expression numerically with $b = 1/a$ and plot the result as a function of $a \in [0, 1]$ in Fig. 8.

References

Artiles W, Carvalho PGS, Kraenkel RA (2008) Patch-size and isolation effects in the Fisher-Kolmogorov equation. J Math Biol 57:521–535

Cantrell R, Cosner C (1999) Diffusion models for population dynamics incorporating individual behavior at boundaries: applications to refuge design. Theor Popul Biol 55:189–207

Cantrell R, Cosner C (2003) Spatial ecology via reaction-diffusion equations. Mathematical and computational biology. Wiley

Cantrell R, Cosner C (2007) Density dependent behaviour at habitat boundaries and the allee effect. Bull Math Biol 69(7):2339–2360

Cantrell R, Cosner C, Fagan W (2012) The implications of model formulation when transitioning from spatial to landscape ecology. Math Biosci Eng 9(1):27–60

Cobbold C, Lewis M, Lutscher F (2005) How parasitism affects critical patch size in a host-parasitoid system: application to Forest Tent Caterpillar. Theor Popul Biol 67(2):109–125

Fagan W, Lutscher F (2006) The average dispersal success approximation: a bridge linking home range size, natal dispersal, and metapopulation dynamics to critical patch size and reserve design. Ecol Appl 16(2):820–828

Frair J, Merrill E, Visscher D, Fortin D, Beyer H, Morales J (2005) Scales of movement by elk (*Cervus elaphus*) in response to heterogeneity in forage resources and predation risk. Landsc Ecol 20:273–287

Hadeler K (2000) Reaction transport equations in biological modeling. Math Comput Model 31:75–81

Hanggi P, Talkner P, Borkovec M (1990) Reaction rate theory: fifty years after Kramers. Rev Modern Phys 62(2):251–342

Hanski I, Ovaskainen O (2000) The metapopulation capacity of a fragmented landscape. Nature 404:755–758

Kierstead H, Slobodkin LB (1953) The size of water masses containing plankton blooms. J Mar Res 12:141–147

Kolpas A, Nisbet R (2010) Effects of demographic stochasiticity on population persistence in advective media. Bull Math Biol 72(5):1254–1270

Kot M (2001) Elements of mathematical ecology. Cambridge University Press, Cambridge

Ludwig D, Aronson DG, Weinberger HF (1979) Spatial patterning of the spruce budworm. J Math Biol 8:217–258

Lutscher F, Lewis MA (2004) Spatially-explicit matrix models. A mathematical analysis of stage-structured integrodifference equations. J Math Biol 48:293–324

Maciel G, Lutscher F (2013) How individual response to habitat edges affects population persistence and spatial spread (Submitted)

Matkowsky B, Schuss Z (1977) The exit problem for randomly perturbed dynamical systems. SIAM Appl Math 33(2):365–382

McKenzie H (2006) Linear features impact predator-prey encounters: analysis with first passage time. Master's thesis, University of Alberta

McKenzie H, Lewis M, Merrill E (2009) First passage time analysis of animal movement and insights into the functional response. Bull Math Biol 71(1):107–129

Othmer H, Adler F, Lewis M, Dallon J (1997) Mathematical modeling in biology: case studies in ecology, physiology and cell biology. Prentice Hall

Ovaskainen O (2008) Analytical and numerical tools for diffusion-based movement models. Theor Popul Biol 73:198–211

Ovaskainen O, Cornell S (2003) Biased movement at a boundary and conditional occupancy times for diffusion processes. J Appl Prob 40(3):557–580

Redner S (2001) A guide to first-passage processes. Cambridge University Press, Cambridge

Samia Y, Lutscher F (2012) Persistence probabilities for stream populations. Bull Math Biol 74(7):1629–1650

Schultz C, Crone E (2001) Edge-mediated dispersal behavior in a prairie butterfly. Ecology 82(7):1879–1892

Shigesada N, Kawasaki K, Teramoto E (1986) Traveling periodic waves in heterogeneous environments. Theor Popul Biol 30:143–160

Singer A, Schuss Z, Osipov A, Holcman D (2008) Partially reflected diffusion. SIAM J Appl Math 28(3):844–868

Skellam JG (1951) Random dispersal in theoretical populations. Biometrika 38:196–218

Strohm S, Tyson R (2012) The effect of habitat fragmentation on cyclic population dynamics: a reduction to ordinary differential equations. Theor Ecol. doi:10.1007/s12080-011-0141-1

Turchin P (1998) Quantitative analysis of movement: measuring and modeling population redistribution of plants and animals. Sinauer, Sunderland

Van Kirk RW, Lewis MA (1997) Integrodifference models for persistence in fragmented habitats. Bull Math Biol 59(1):107–137

Van Kirk RW, Lewis MA (1999) Edge permeability and population persistence in isolated habitat patches. Nat Resour Model 12:37–64

Vasilyeva O, Lutscher F (2012) Competition of three species in an advective environment. Nonlinear Anal: Real World Appl 13(4):1730–1748

Wakano J, Ikeda K, Miki T, Mimura M (2011) Effective dispersal rate is a function of habitat size and corridor shape: mechanistic formulation of a two-patch compartment model for spatially continuous systems. Oikos 120(11):1712–1720

Weins J, Stenseth N, Van Horne B, Ims R (1993) Ecological mechanisms and landscape ecology. Oikos 66:369–380